ARTICLES
PUBLISHED ONLINE: 4 SEPTEMBER 2011 | DOI: 10.1038/NMAT3096
nature materials

Large variation of vacancy formation energies in the surface of crystalline ice

M. Watkins[1,2,3], D. Pan[4], E. G. Wang[5], A. Michaelides[1,2,3], J. VandeVondele[6] and B. Slater[1,3]*

Resolving the atomic structure of the surface of ice particles within clouds, over the temperature range encountered in the atmosphere and relevant to understanding heterogeneous catalysis on ice, remains an experimental challenge. By using first-principles calculations, we show that the surface of crystalline ice exhibits a remarkable variance in vacancy formation energies, akin to an amorphous material. We find vacancy formation energies as low as ∼0.1–0.2 eV, which leads to a higher than expected vacancy concentration. Because a vacancy's reactivity correlates with its formation energy, ice particles may be more reactive than previously thought. We also show that vacancies significantly reduce the formation energy of neighbouring vacancies, thus facilitating pitting and contributing to pre-melting and quasi-liquid layer formation. These surface properties arise from proton disorder and the relaxation of geometric constraints, which suggests that other frustrated materials may possess unusual surface characteristics.

Despite ice being a ubiquitous and well-studied substance, it is surprising that some basic questions about its properties and structure are still debated. For example, Faraday contentiously proposed that the surface of hexagonal ice (Ih) was liquid-like to explain a 'regelation' experiment conducted in the 1850s (ref. 1), but some 160 years later the pre-melting mechanism, structure, and temperature dependence of the quasi-liquid layer is an unresolved problem. In another example, until recently it has been thought that ice particles in clouds exclusively existed in the hexagonal phase, but emerging evidence suggests that the cubic ice phase may be present in significant concentrations[2]. Remarkably, it has been found just very recently that water freezes differently on positively and negatively charged surfaces[3]. The first two examples are especially relevant to atmospheric chemistry; ice particles within high-altitude cirrus clouds are known to catalyse the formation of HOCl radicals, which cause the destruction of ozone in the polar regions[4] and other trace gas reactions[5,6]. Hexagonal ice covers up to 15% of the planet at the boundary layer[7] and ≳50% of the earth is covered in ice cloud[8]. Cloud coverage is linked to climate regulation through albedo and geochemical cycling, which feed back into climate patterns. A major obstacle to better understanding cloud microphysics and nanoscale atmospheric chemistry within clouds is the lack of an atomistic picture of the surface structure of ice.

Following on from our recent investigations, which have revealed that the surface of ice has a surprisingly ordered arrangement of water molecule orientations[9–11] and that ionic defects may acidify the ice surface[12], we report a study of the important molecular vacancy defect. Whereas vacancies within the crystal interior have been studied previously by theoretical approaches[13] and the connection between vacancies and proton conduction discussed[14], to our knowledge surface vacancies have not been explicitly examined before. Here, we show that the surface of crystalline ice exhibits a remarkable variation in vacancy formation energies, redolent of an amorphous rather than a crystalline material. Indeed, a significant proportion of water molecules at the ice surface are bound by the equivalent of a hydrogen bond fewer than most molecules in the same layer. The strong connection of these findings to the reactivity (in terms of heterogeneous catalysis by ice), pre-melting, and growth of ice is discussed in detail.

As this work focuses on the energy to create individual water molecule vacancies at the surface of an ice crystal, we begin with a consistency check of our computational methodology for vacancy formation in the bulk of the ice crystal. With our chosen computational set-up (see Supplementary Information for details) the average vacancy formation energy, the energy to take one water molecule out of an ice crystal and place it in a bulk site, is +0.74 eV with a maximum deviation of ±0.025 eV. This value and the very small standard deviation in the bulk vacancy formation energy are consistent with the work of de Koning[13].

Moving to the surface, we show the structure used to model the (0001) crystalline surface of ice Ih in Fig. 1. Our ice slab consists of six bilayers (see Supplementary Information S1)—planes separated by ∼0.9 Å with an inter-bilayer separation of ∼2.8 Å. The outermost part of the bilayer (labelled 1 and coloured red) has molecules with one dangling hydrogen bond (formally, three hydrogen bonds in total), whereas the inner part of the bilayer (and all other layers) has no dangling bonds (formally, four hydrogen bonds in total per molecule). From this surface model, individual water molecules were selected and removed from the slab, and subsequently the surface was allowed to relax. In Fig. 2, we show the single vacancy formation energies of over 40 unique water molecules sampled from all layers of the slab. Figure 2 exhibits a number of important and noteworthy features. First, we note that vacancy formation is always endothermic and that the energy of the vacancies generally increases as one moves from the crystal exterior (layers 1 and 2) to the interior (layers 5 and 6). This indicates that vacancies formed at the surface will not migrate to the interior at moderate temperatures and that the concentration of surface vacancies in the first one or two bilayers will be far

[1]Department of Chemistry, Christopher Ingold Building, 20 Gordon Street, University College London, London WC1H 0AJ, UK, [2]London Centre for Nanotechnology, University College London, London WC1H 0AJ, UK, [3]TYC@UCL, University College London, London WC1H 0AJ, UK, [4]Institute of Physics, Chinese Academy of Sciences, PO Box 603, Beijing 100190, China, [5]School of Physics, Peking University, Beijing 100871, China, [6]Institute of Physical Chemistry, University of Zurich, Winterthurerstrasse 190, CH-8057 Zurich, Switzerland. *e-mail: b.slater@ucl.ac.uk.

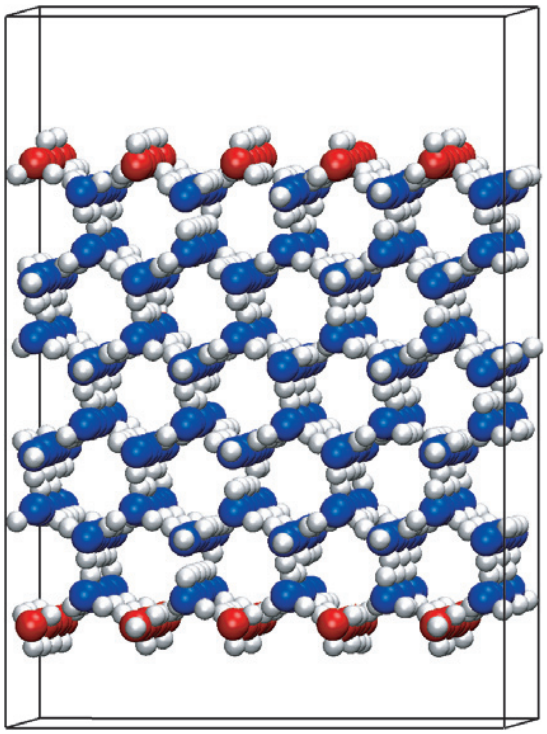

Figure 1 | The ice Ih {0001} surface. This cell was used to compute vacancy energies and dipole moments, and consists of a 360-molecule slab with dimensions 22.15 × 23.02 × 31.55 Å, containing a 10 Å vacuum gap perpendicular to the surface. Ice has a bilayer structure—this slab consists of 12 individual layers or six bilayers, each bilayer consisting of 60 molecules. Red water molecules formally have three hydrogen bonds whereas blue water molecules have four hydrogen bonds.

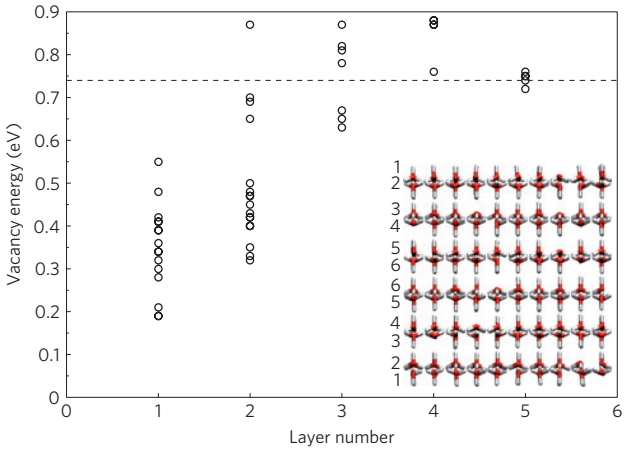

Figure 2 | Distribution of vacancy formation energies in an ice slab. Vacancy formation energies computed for a 6-bilayer slab of (0001) ice Ih (containing 12 layers in total). The inset figure corresponds to the configuration in Fig. 1, but viewed along the [010] axis, that is, in cross-section. Layer 1 is the external layer containing undercoordinated water molecules. Layer 2 molecules notionally have four hydrogen bonds per water. The vacancy energy generally increases as a function of the depth into the crystal. The dashed line indicates the vacancy formation energy (0.74 eV) for the crystal bulk. Note that the variance in vacancy energy in the bulk is 0.025 eV, and hence the dashed-line width overemphasizes the variance.

greater than that in the interior. More remarkably, we find that the vacancy formation energies vary by ∼0.8 eV (∼80 kJ mol^{-1}), with a proportion of the water molecules having formation energies of less than 0.2 eV. This is a surprisingly large variation in vacancy formation energies, approximately 30 times greater than the 0.025 eV variance seen in the bulk, and much larger than the typical energy scale associated with proton disorder effects in the bulk or at the surface[9–11]. We also find molecules in layer 2 within the crystal exterior that are more strongly bound (∼0.9 eV) than any of those found in the crystal interior, which is consistent with previous studies of more amorphous nanoparticulate ice[15]. Indeed, a sizeable fraction of molecules in layer 1 with three notional hydrogen bonds are more strongly bound than those in layer 2 with four notional hydrogen bonds. As each molecule in hexagonal ice sits on a regular hexagonal crystal lattice site, one might expect that the binding energies would be approximately equal, as is found in the crystal interior, but the pronounced variance seen here is unprecedented in our experience, for crystalline materials.

Let us now try to understand why such a large variation in surface vacancy formation energies is observed. To begin, we sought to examine how the electrostatic properties of each molecule vary by investigating the dipole moment of each molecule within the whole slab using Wannier centres, in a similar manner to previous work[16]. In Fig. 3, we plot the molecular dipole moments obtained from two different faces of hexagonal ice: the basal plane discussed already and also the prismatic (10–10) face, another important surface frequently exposed on ice crystallites. Whereas the molecules within interior layers of each slab have a narrow distribution of dipole moments of around 3.5 ± 0.1 D, at the exterior layers the variance is unexpectedly large, falling in the range 2.9–4.4 D. Molecules in the outer part of the bilayer have a lower average dipole moment of 3.23 D (in the range ∼2.9–3.6 D) in comparison to those immediately below the coordinatively unsaturated layer, which have an average dipole moment of 3.52 D, approximately equal to the bulk value, albeit with a very large range of ∼3.1–4.4 D. As was seen for the vacancy energies, a strong variance is seen in the surface layers, which confounds expectation for a crystalline ice phase. For comparison, dipole moments obtained from a relaxed slab of low-density amorphous (LDA) ice were computed and are shown in Supplementary Information S2. Indeed, crystalline ice surfaces resemble amorphous ice in that the LDA surface dipole moments vary considerably (∼2.6–3.8 D) but the interior of crystalline ice and LDA ice are distinct; the moment distribution in bulk is ∼3.0–3.75 D for LDA ice, much larger than the distribution of 3.5 ± 0.1 D found for crystalline ice. As both dipole moments and vacancy energies show great variance, it is interesting to ask if they are correlated. Figure 4 confirms a reasonable general correlation between vacancy energies and dipole moments that shows that weakly bound molecules can be readily identified by small dipole moments. Indeed, Fig. 4 shows that molecules with dipole moments of around 2.7 D will have binding energies approaching zero. Approximately 10% of molecules in the external surface layer are underbound by more than the equivalent of one hydrogen bond, hence microscopic ice particles will contain significant concentrations of exceedingly weakly bound water molecules, which would be easily displaced onto the outer layer at moderate temperatures.

We now briefly consider why such large variations in dipole moments are observed, focussing on the molecules in the topmost layer. In Fig. 5 the spatial distribution of dipole moments at the surface is reported, where it can be seen that there is no simple electrostatic compensation mechanism in operation, that is, large dipoles are not found exclusively hydrogen-bonded to molecules with small dipole moments. It is also clear that the extrema of dipole moments are reasonably homogeneously distributed over the surface; molecules with low dipole moments are not clustered together and neither are molecules with large dipole moments. The origin of this distribution can be rationalized by noting that

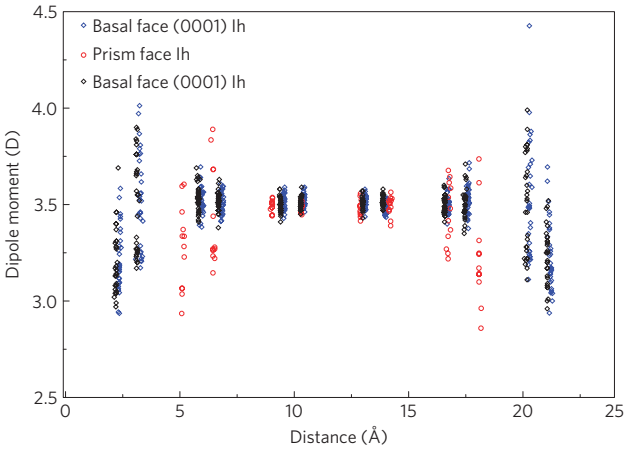

Figure 3 | Dipole-moment distribution in ice slabs. The dipole moment of individual molecules within two 6-bilayer slabs of ice Ih exposing the (0001) surface, and within a 4-bilayer slab exhibiting the prismatic face. The two different samples for the basal face correspond to slabs with different degrees of proton disorder at the surface. In the interior of the crystal slab, the dipole moment is approximately 3.5 Debye, but for all the structures considered here the dipole moments vary greatly towards, and at, the crystal surface.

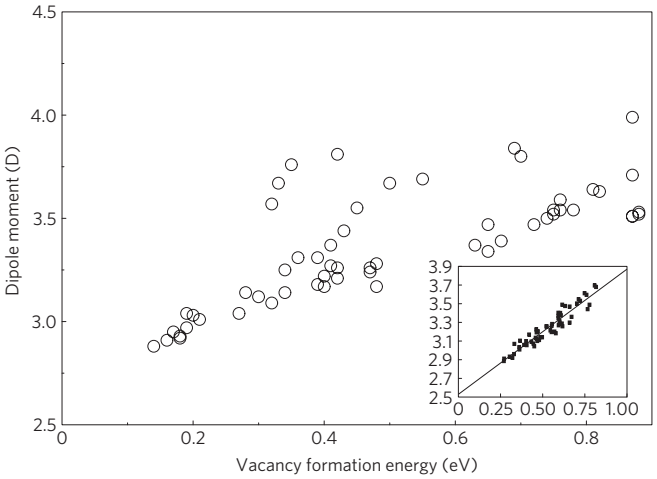

Figure 4 | Correlation between vacancy formation energies and dipole moments. Scatter plot of the dipole moments and associated vacancy formation energies calculated for over 50 unique sites within a 6-bilayer Ih slab that exposes (0001) surfaces, showing a general positive correlation between dipole moment and vacancy formation energy. The inset is a plot of the unrelaxed defect formation energy versus dipole moment with same axis labels as the main figure.

there are electric fields at the ice surface that arise from the inhomogeneous distribution of effective charges at the surface. The effective charges are those associated with the uncoordinated H atoms of the water molecules in the top layer (that is, the dangling protons) and the dangling lone pairs[10]. Particular arrangements of dangling protons and lone pairs create local electric fields that can either enhance or reduce the dipole moment of a molecule in their vicinity. For example, in Fig. 5b a situation is shown where the spatial arrangement of dangling protons produces a local electric field that opposes the intrinsic dipole moment of the water molecule, leading to a lowering of the dipole moment of the molecule in question. As another example, the opposite scenario is shown in Fig. 5c, where the local electric field produced by the dangling protons is aligned with the dipole moment of the central water such that its dipole is enhanced. The same basic argument can effectively be extended to the subsurface layers.

We now turn to the ramifications of our findings. Our calculations show that many water ice molecules at the surface are very weakly bound, and these will give rise to a multitude of surface vacancies. These vacancies have the potential to act as traps of differing strength or depth; to explore how the traps might take up adsorbates, we focus on reactions of the type $X_{(g)} + H_2O^{N}_{(surf)} \rightarrow H_2O_{(admolecule)} + [H_2O^{N-1}_{(surf)} \cdot X_{(surf)}]$; that is, the liberation of a water from the surface layer to form an admolecule above the surface (yielding a surface vacancy) and the adsorption of a gaseous molecule X within the trap. Here, we have selected adsorbates to probe the electrostatic and steric properties of the vacancy trap sites: polar HF has approximately the same dipole moment as H_2O and is emitted at the boundary layer from volcanoes on earth; HF is known to be relatively soluble in ice and relevant to cosmochemistry (for example, it is an important component in the cryosphere of Venus[17]); H_2S, also emitted from volcanoes, has a similar shape to H_2O, but smaller dipole, and ammonia is an air pollutant with low dipole. We also consider HCl, which is an important stratospheric gas implicated in ozone destruction, noting that its adsorption behaviour is complex and the subject of conflicting experimental and theoretical studies (refs 5, 6 and refs therein). In Fig. 6, the overall cost of the reaction is shown for the gases considered, along with water, for reference. For HF and HCl, the reaction energy exceeds that of water for all but the most weakly bound water molecules, indicating that these gases will attack, and be incorporated into the ice surface, in agreement with experimental studies (ref. 7 and refs therein). In addition, the reaction energy for these two gases is strongly correlated with the vacancy formation energy. Water molecules with large dipole moments are strongly bound, but HF and HCl bind more strongly than water at most surface sites and are expected to displace water molecules at sites that would not be expected to form intrinsic vacancies. Extrapolation and comparison of the lines for water and ammonia suggest that at very shallow traps, that is, low energy vacancies, water could be vulnerable to displacement by ammonia in low partial pressures of H_2O. Unlike HF and HCl, ammonia is relatively insensitive to the trap depth because of its small dipole moment. H_2S will not displace water and shows a weak inverse correlation between reaction energy and well depth. All the molecules show strong binding to the vacancy (see Supplementary Fig. S3), but free water would, for example, displace H_2S.

Finally, we consider how the existence of weakly bound water molecules on the ideal surface relates to the pre-melting phenomenon. In Supplementary Fig. S4, a single weakly bound water was removed from one side of the slab and the dipole moments recomputed. The dipole moments of molecules in the external part of the surface are reduced, thus weakening the binding of molecules to the crystal. The dipole is related to the number of hydrogen bonds and, hence, by breaking three hydrogen bonds the dipole moment of several molecules decreases. The effect is emphasized if molecules are removed in a stepwise fashion to create di-, tri-, quad- and quin-vacancies similar to those studied by Buch *et al.*[18]; we find that the successive energies to form the vacancy complexes are 0.19, 0.28, 0.09, 0.18 and 0.15 eV from the initial vacancy to the quin-vacancy complex respectively. These energies should be contrasted with the energies for the formation of the individual vacancies of 0.19, 0.46, 0.44, 0.67 and 0.42 eV. This finding suggests a cascade mechanism, whereby once a low-energy vacancy is created, neighbouring molecules become very weakly bound, with the potential to lead to the growth of pits and increased concentrations of very mobile surface-adsorbed species. We make the suggestion here that this is a mechanism that could aid the formation of quasi-liquid layers at the surface. Exploratory *ab initio* molecular dynamics runs presented in the Supplementary Information confirm the high mobility of

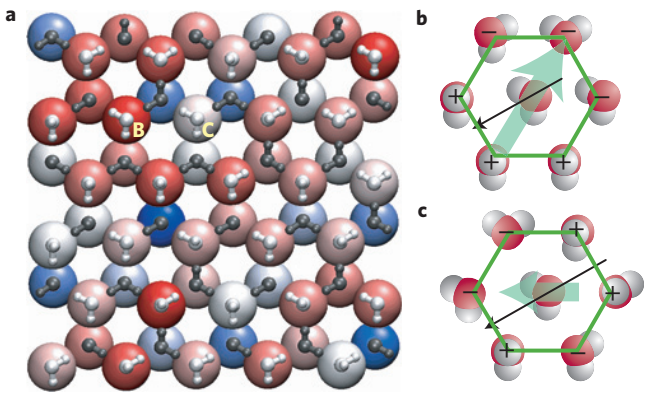

Figure 5 | Spatial variation of dipole magnitude. a, A top view of the spatial distribution of dipole moments for the (0001) surface of ice Ih (equivalent to layer 1 and 2 in Fig. 1). The image is a composite, where the magnitude of the water dipole is represented by a coloured sphere; red indicates a low dipole, white an intermediate dipole, and blue a large dipole. The ball-and-stick water molecules are superimposed on the spheres, where layer 1 molecules are in white and layer 2 molecules are in grey. **b**,**c** Two specific examples taken from the points marked B and C in **a**, respectively, indicate how local electric fields (denoted by light green arrows) created by the net effective charges on the dangling protons (+ve) and dangling lone pairs (−ve) can either reduce (**b**) or enhance (**c**) the dipole moments (indicated by black arrows) of molecules in the top layer. Note that the layer 2 molecules have been hidden in **b** and **c** to emphasize the surface geometry.

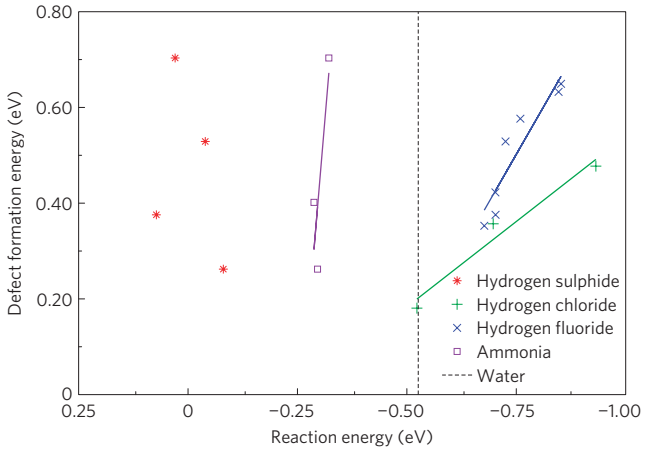

Figure 6 | Reactivity of various gases at surface vacancies. The figure shows the substitution reaction energy for HF, HCl, H_2S and NH_3 with water molecules at the (0001) surface of ice. The vacancy formation energy reflects how strongly the water molecule is bound. The reaction energy corresponds to the energy released on displacement of a water molecule at the surface to an atop location. The dashed line signifies the attack of a gaseous water molecule at a surface site and displacement of a water to an atop location. Right of the dashed line indicates displacement of surface bound water in a competitive reaction between a gas molecule and gaseous water. Negative reaction energies indicate displacement of surface bound water when the partial pressure of gaseous water is low.

weakly bound molecules that give rise to surface admolecules. In addition, in the Supplementary Information we provide evidence that increased proton disorder, which occurs with increasing temperature, causes a weakening of all surface hydrogen bonds, including those of the least strongly bound molecule, suggesting that weakly bound molecules can be thermally activated.

To summarize, we find a remarkable variance in the vacancy formation energy at the external surface of ice. Approximately 10% of surface molecules are very weakly bound, yet other sites are more strongly bound than those in the crystal interior. This variation in binding is most unusual for a crystalline system and can be compared to a pocket-sprung mattress where each spring has a unique tension. In a chemical context, this finding suggests that the number of surface vacancy sites will be far greater than one would expect in the crystal bulk for this crystalline material. This finding may explain the variation in, and high vapour pressure of, ice samples[19]. Moreover, the vacancies will have a spectrum of trapping energies such that the reaction energy landscape of, for example, a trace gas molecule in the vicinity of one trap could be markedly different from another, similar to what has been observed for ice nanoparticles[20]. More generally, the crystalline ice surface can be expected to be more reactive than previously thought, owing to the abundance of vacancy traps and the varied polarity of surface sites. The availability of loosely bound water molecules at the surface also suggests a potential contribution to the mechanism of pre-melting and quasi-liquid layer formation. Simulations reported here show the formation of surface vacancies and a germinal quasi-liquid layer, significantly below the bulk melting temperature, as has been previously reported using force-field modelling approaches[9,21,22]. The activation energy for vacancy migration in the bulk has been measured to be ∼0.62 eV (ref. 7 and refs therein) and the vacancy energy to be 0.53 eV. The surface vacancy formation energies of ∼0.2 eV predicted here suggest that the thermal conductivity of the external layers through vacancy diffusion should be enhanced (and presumably, electrical conductivity increased). Measurements of self-diffusion between H_2O and D_2O in the outer layers of ice suggest a diffusion energy barrier of ∼0.1 eV (ref. 23), remarkably close to our computed vacancy formation energy at the crystalline ice surface. Enhanced reactivity has been noted on ice surfaces, such as photolysis of aromatic hydrocarbons, which is not observed on water[24], albeit at temperatures where the quasi-liquid layer is present. Sum frequency generation studies by Groenzin *et al.* on Ih ice samples show a broad range of frequencies on the surface for the OH stretch at around 3,100 cm^{-1} (ref. 25). Buch and Devlin[26] showed that a model which considered proton disorder and local oscillations of dipole moments around each water molecule in the bulk (where dipole moments are very similar) helped to explain vibrational signatures of crystalline ice. At the surface, there is a much greater disparity in dipole moment around each water molecule and hence, by extrapolation of the Buch and Devlin findings, a large broadening of surface signals is expected because of more pronounced oscillations in the local electric field gradient.

Finally, the presence of water molecules within terraces that have very varied binding energies may have ramifications for crystal growth and dissolution, as well as catalysis. Ordinarily, in the classic Kossel picture of crystals, each surface site on a terrace is considered to be equivalent, but here we find molecules within the topmost layer that are bound by more than the equivalent of one hydrogen bond in comparison to other molecules found in the same layer. Molecules destined for shallow traps in growth may be more prone to misalignment, which may help to explain the very high density of dislocations observed in ice samples (ref. 7 and refs therein, ref. 27). In the context of catalysis, a spectrum of reactivity is seen in other materials only through a range of coordinatively distinct sites, such as steps and kinks and a range of exposed crystal faces, but in ice this is possible on a single terrace.

More broadly, ice is the archetypal frustrated material; unlike in magnetic spin ices[28] the frustration is electrostatic in origin, owing to the interaction of molecular dipoles within local electric fields arising from a disordered array of dipoles. We see here that because of the relaxation of geometric constraints at the surface, unexpected surface properties are observed—suggesting that surfaces of other frustrated materials could have unforeseen properties.

Methods

Calculations were carried out using the Quickstep module of the CP2K program suite[29]. Quickstep is a very efficient implementation of Density Functional Theory using a novel dual basis technique of localized Gaussians and plane waves. In our calculations the plane wave cutoff was 300 Ry, appropriate to the Goedecker–Teter–Hutter (GTH, refs 30,31) pseudopotentials we employed, and the localized basis set was of triple zeta plus double polarization (TZV2P) quality, sufficient to reduce the basis set superposition error of a water dimer to <15 meV. Calculations were performed using the Perdew–Burke–Ernzerhof (PBE) exchange correlation functional[32] and structures were considered relaxed when forces were less than 25 meV Å^{-1}.

For bulk simulations a 96-molecule supercell was used, whereas to simulate the surface, a 360-molecule cell that consisted of six water bilayers and surface plane dimensions 22.15 × 23.02 Å was employed. These pseudo-orthorhombic cells were taken from the work of Hayward and Reimers[33] and have the desirable properties of maximal proton disordering (which yields a low energy, anti-ferroelectric cell) and zero dipole moment, which is vital for the periodic approach used here. The bulk lattice constants were optimized, leading to a and c values of 4.430 and 8.185 Å respectively, in good agreement with reference plane wave calculations. Similarly, the lattice energy of ice was found to be 0.698 eV, in good agreement with high quality plane wave calculations[34] and identical for both 96- and 360-molecule cells. For simulations of the surface, a vacuum gap of 10 Å was introduced into the cell, which was sufficient to reduce spurious interaction between images below 5 meV in the total energy of 1,080 atoms. The check was performed by calculating the energies of the relaxed surface using a 2D Poisson solver[35]. In the Supplementary Information we give extensive information about tests performed to address finite size effects, the influence of the exchange–correlation functional (including both the generalized gradient approximation and a hybrid functional), quantum effects, the surface proton order parameter and van der Waals interactions.

Received 1 October 2010; accepted 11 July 2011; published online 4 September 2011

References

1. Faraday, M. On certain conditions of freezing water. *Athenaeum* **1181,** 640–641 (1850).
2. Murray, B. J., Knopf, D. A. & Bertram, A. K. The formation of cubic ice under conditions relevant to Earth's atmosphere. *Nature* **434,** 202–205 (2005).
3. Ehre, D. *et al.* Water freezes differently on positively and negatively charged surfaces of pyroelectric materials. *Science* **327,** 672–675 (2010).
4. Molina, M. J. Polar ozone depletion. *Angew. Chem. Int. Ed.* **35,** 1778–1785 (1996).
5. Abbatt, J. P. D. Interactions of atmospheric trace gases with ice surfaces: Adsorption and reaction. *Chem. Rev.* **103,** 4783–4800 (2003).
6. Huthwelker, T., Ammann, M. & Peter, T. The uptake of acidic gases on ice. *Chem. Rev.* **106,** 1375–1444 (2006).
7. Petrenko, V. F. & Whitworth, R. W. *Physics of Ice* (Oxford Univ. Press, 2002).
8. http://neo.sci.gsfc.nasa.gov.
9. Bishop, C. *et al.* On thin ice: Surface order and disorder during pre-melting. *Faraday Discuss.* **141,** 277–292 (2009).
10. Pan, D. *et al.* Surface energy and surface proton order of ice Ih. *Phys. Rev. Lett.* **101,** 155703 (2008).
11. Pan, D. *et al.* Surface energy and surface proton order of the ice Ih basal and prism surfaces. *J. Phys. Condens. Matter* **22,** 074209 (2010).
12. Watkins, M., VandeVondele, J. & Slater, B. Point defects at the ice (0001) surface. *Proc. Natl Acad. Sci. USA* **107,** 12429–12434 (2010).
13. de Koning, M., Antonelli, A., da Silva, A. J. R. & Fazzio, A. Structure and energetics of molecular point defects in ice I-h. *Phys. Rev. Lett.* **97,** 155501 (2006).
14. de Koning, M. & Antonelli, A. Modeling equilibrium concentrations of Bjerrum and molecular point defects and their complexes in ice I-h. *J. Chem. Phys.* **128,** 164502 (2008).
15. Buch, V., Bauerecker, S., Devlin, J. P., Buck, U. & Kazimirski, J. K. Solid water clusters in the size range of tens-thousands of H_2O: A combined computational/spectroscopic outlook. *Int. Rev. Phys. Chem.* **23,** 375–433 (2004).
16. Tribello, G. A. & Slater, B. Proton ordering energetics in ice phases. *Chem. Phys. Lett.* **425,** 246–250 (2005).
17. Bertaux, J. L. *et al.* A warm layer in Venus' cryosphere and high-altitude measurements of HF, HCl, H_2O and HDO. *Nature* **450,** 646–649 (2007).
18. Buch, V., Delzeit, L., Blackledge, C. & Devlin, J. P. Structure of the ice nanocrystal surface from simulated versus experimental spectra of adsorbed CF_4. *J. Phys. Chem.* **100,** 3732–3744 (1996).
19. Fray, N. & Schmitt, B. Sublimation of ices of astrophysical interest: A bibliographic review. *Planet. Space Sci.* **57,** 2053–2080 (2009).
20. Devlin, J. P., Uras, N., Sadlej, J. & Buch, V. Discrete stages in the solvation and ionization of hydrogen chloride adsorbed on ice particles. *Nature* **417,** 269–271 (2002).
21. Conde, M. M., Vega, C. & Patrykiejew, A. The thickness of a liquid layer on the free surface of ice as obtained from computer simulation. *J. Chem. Phys.* **129,** 14702–14711 (2008).
22. Neshyba, N., Nugent, E., Roeselova, M. & Jungwirth, P. Molecular dynamics study of ice–vapor interactions via the quasi-liquid layer. *J. Phys. Chem. C* **113,** 4957–4604 (2009).
23. Kang, H. Chemistry of ice surfaces. Elementary reaction steps on ice studied by reactive scattering. *Acc. Chem. Res.* **38,** 893–900 (2005).
24. Kahan, T. F. & Donaldson, D. J. Photolysis of polycyclic aromatic hydrocarbons on water and ice surfaces. *J. Phys. Chem. A* **111,** 1277–1285 (2007).
25. Groenzin, H. *et al.* The single-crystal, basal face of ice I_h investigated with sum frequency generation. *J. Chem. Phys.* **127,** 214502 (2007).
26. Buch, V. & Devlin, J. P. A new interpretation of the OH-stretch spectrum of ice. *J. Chem. Phys.* **111,** 3437–3443 (1999).
27. Sazaki, G. *et al.* Elementary steps at the surface of ice crystals visualized by advanced optical microscopy. *Proc. Natl Acad. Sci. USA* **107,** 19702–19707 (2010).
28. Harris, M. J. *et al.* Geometrical frustration in the ferromagnetic pyrochlore $Ho_2Ti_2O_7$. *Phys. Rev. Lett.* **79,** 2554–2557 (1997).
29. VandeVondele, J. *et al.* QUICKSTEP: Fast and accurate density functional calculations using a mixed Gaussian and plane waves approach. *Comput. Phys. Commun.* **167,** 103–128 (2005).
30. Goedecker, S., Teter, M. & Hutter, J. Separable dual-space Gaussian pseudopotentials. *Phys. Rev. B* **54,** 1703–1710 (1996).
31. Krack, M. Pseudopotentials for H to Kr optimized for gradient-corrected exchange–correlation functionals. *Theor. Chem. Acc.* **114,** 145–152 (2005).
32. Perdew, J. P., Burke, K. & Ernzerhof, M. Generalized gradient approximation made simple. *Phys. Rev. Lett.* **77,** 3865–3868 (1996).
33. Hayward, J. A. & Reimers, J. R. Unit cells for the simulation of hexagonal ice. *J. Chem. Phys.* **106,** 1518–1529 (1997).
34. Hu, X. L. & Michaelides, A. Water on the hydroxylated (001) surface of kaolinite: From monomer adsorption to a flat 2D wetting layer. *Surf. Sci.* **602,** 960–974 (2008).
35. Genovese, L., Deutsch, T. & Goedecker, S. Efficient and accurate three-dimensional Poisson solver for surface problems. *J. Chem. Phys.* **127,** 054704 (2007).

Acknowledgements

We thank EPSRC for funding M.W. through the grant A Quickstep Forward: Development of the CP2K/Quickstep Code and Application to Ice Transport Processes EP/F011652/1. B.S. wishes to thank R. Martonak for supplying coordinates of amorphous ice phases and S. Bramwell for useful discussions. D.P. and E.G.W. are supported by NSFC. D.P. is grateful to the Thomas Young Centre (www.thomasyoungcentre.org) for a Junior Research Fellowship. A.M. is also supported by the EURYI scheme (www.esf.org/euryi), the EPSRC, and the European Research Council. Computational resources from the London Centre for Nanotechnology and UCL Research Computing are warmly acknowledged. Also via our membership of the UK's HPC Materials Chemistry Consortium, which is funded by EPSRC (EP/F067496), this work made use of the facilities of HECToR, the UK's national high-performance computing service. J.V.V. acknowledges computer resources from the Swiss National Supercomputing Centre (CSCS).

Author contributions

B.S., M.W. and J.V.V. designed the research. Most of the calculations were performed by M.W. with contributions from all authors. All authors contributed to the analysis and discussion of the data and the writing of the manuscript.

Additional information

The authors declare no competing financial interests. Supplementary information accompanies this paper on www.nature.com/naturematerials. Reprints and permissions information is available online at http://www.nature.com/reprints. Correspondence and requests for materials should be addressed to B.S.